J Mater Sci (2007) 42:1010–1018
DOI 10.1007/s10853-006-1384-x

# Synthesis of tungsten bronze powder and determination of its composition

**Meirav Mann · Gennady E. Shter · George M. Reisner · Gideon S. Grader**

Received: 27 July 2004 / Accepted: 13 January 2006 / Published online: 28 December 2006


**Abstract** Sodium tungsten bronze powders were synthesized by thermal reduction of a gas/melt system at high temperature. Samples having a cubic structure with different compositions were prepared. The initial melt included $Na_2WO_4$, $WO_3$ and 10–40% mol. NaCl while the reducing gas was hydrogen at 750 °C. An original mechanism of controlling the powders size and distribution was suggested and discussed. A quantitative novel and simple method to determine the bronze composition based on TGA data was developed. An increase in the NaCl content led to a decrease of the crystals size and improved the powder uniformity. Fine powders, in the 2–5 μm size range, were synthesized from melt with 40% mol of NaCl. The stoichiometry parameter $x$ of the obtained bronzes ranged from 0.8 to 0.92. An excellent agreement between $x$ values determined by the classical XRD route and the proposed TGA method was demonstrated.

## Introduction

Oxide bronzes, have received intensive attention in the past years [1–11]. These materials are known as non-stoichiometric compounds with a general formula of $M_xAO_y$, where M is an electropositive metal such as an alkali, alkaline earth or a rare earth metal, A is a transition element such as tungsten, molybdenum, vanadium, etc., and $x$ varies between 0 and 1 depending on the formal oxidation state of A. Bronzes exhibit a rich crystal chemistry and a wide range of electrophysical properties. The high metallic-type electrical conductivity observed for large values of $x$ and the possibility of varying the composition over a wide range, gave rise to many investigations concerning the structural and physical properties of tungsten bronzes [2].

Most investigations in this field were dedicated to tungsten bronzes $M_xWO_3$, where M is mainly Na or K [2]. Tungsten oxide bronzes were the first to be reported, as early as 1823, by Wöhler. The designation ''wolframbronce'' was originally introduced by Philipp and Schwebel [1] to describe the yellow, metallic luster of $Na_xWO_3$ ($x$ = 0.8), though the term was also applied to the purple-red ($x$ = 0.6) and blue ($x$ = 0.4) materials.

Most of the research has been dedicated to single crystal bronzes and their growth and/or polycrystalline materials, with relatively large crystals. Emphasis was laid on the electrochemical preparation method, in which an electrical current reduces a melt mixture of $MWO_4$ and $WO_3$ [7–10, 12]. The main disadvantage is the low reproducibility of $x$ due to changes in composition, density, viscosity and electrical conductivity of the electrolyte during the electrolysis process. Another problem in some applications is the formation of large crystals of 5–400 microns [13].

Chemical methods are in general based on the syntheses of bronzes from tungstates, $WO_3$ and different additives such as metaphosphates, chlorides, etc. in the presence of a reducing agent [12]. In most of these

M. Mann · G. E. Shter · G. S. Grader (✉)
Chemical Engineering Department, Technion, Haifa 32000, Israel
e-mail: grader@tx.technion.ac.il

G. M. Reisner
Crown Center for Superconductivity and Physics Department, Technion, Haifa 32000, Israel

cases fine powdered metallic tungsten is used for high temperature reduction of tungstates in solids or melts [9, 13, 14]. One of the main obstacles here is product non-uniformity due to processing difficulties. A relatively new route for the synthesis of tungsten oxide bronzes involved ambient temperature reduction of aqueous solutions of $NaBH_4$ and $Na_2WO_4$. Sodium borohydride acts as a reducing agent, yielding a gel of reduced sodium tungsten oxide and finally crystalline sodium tungsten bronze after heat treatment [15, 16]. The disadvantages of this method are as following: (a) the process includes several complicated steps and needs a careful adjusting of parameters, (b) a high cost of the reducing agent and (c) a low yield of the final product.

The use of tungsten bronzes as heterogeneous catalysts has been proposed. This possibility stems from the affinity of the bronzes for oxygen atom recombination, which involves an electron transfer between adsorbate and adsorbent. This process is composition-dependent, which brings about issues of product uniformity. Catalytic activities were found to be closely related to the electronic properties of the bronzes [17]. The electrocatalytic activity of cubic sodium tungsten bronze has been demonstrated. Intentional platinization of the bronze electrode (as Pt or $PtWO_3$) provided an electrocatalytic activity similar to platinum towards the cathodic reduction of oxygen, especially in an acid electrolyte [18, 19].

An oxygen electrode for a fuel cell utilizing an acid electrolyte, has a substrate of an alkali metal tungsten bronze, which is covered with a thin layer of platinum tungsten bronze having the formula $Pt_yWO_3$, where $y$ is at least 0.5. The electrocatalyst electrode is prepared by replacing the surface alkali metal with platinum to form $Pt_yWO_3$. The prepared electrode has a catalytic activity equal to platinum electrodes, but contains less platinum than most other such electrodes and is therefore less expensive, and was found to be more corrosion resistant than most platinum metal electrodes. The electrode is suitable for use in fuel cells, which utilize an acid electrolyte such as sulfuric acid or phosphoric acid, and may be used as the oxygen (cathode) electrode [20].

The bronze acts as construction material of electrodes for special applications, for example: the continuous determination of the carbon monoxide content in the air in the emission range, and comprises an electrochemical cell including an acid electrolyte. The cathode includes sodium tungsten bronze as a conductivity additive, which increases the electrode activity, and gives rise to a linear dependence of the current on the carbon monoxide concentration [21].

Another category of electrodes, where tungsten bronzes play a role, is electroanalytical chemistry. These types of electrodes are used as indicators in different electrochemical systems. Shanks et al. [20] showed that the bronze electrode may be used to determine pH, p[metal] for certain reducible species such as Ag, Hg, and to follow the potential change involved in some oxidation–reduction systems [22]. The bronze electrode could function as a potentiometric indicating electrode for dissolved oxygen in aqueous solutions. This application can be beneficial in the environmental field, resulting from the large sensitivity and magnitude of the potential change per unit variation of the oxygen concentration [23].

A special application of sodium tungsten bronzes is as source of sodium ions in electrolysis. This application is based on the reversibility of sodium tungsten bronzes to sodium ions, which was used to measure the diffusion of these ions in beta-alumina and in the bronze structure itself [24].

In the above-mentioned applications, some of the important parameters are the particle's size, their distribution and their stoichiometry. These topics are the central issues of the current investigation.

The first goal of the present work was to synthesize fine bronze powder, with controlled size and composition, via reduction of tungsten salts/oxides concentrated melts by gaseous agents.

Due to the dependence of the properties of the bronze on its composition, an accurate determination of the value of $x$ is highly important. An analytical chemical method for the determination of the sodium content (the value of $x$) in bronzes is the van Duyn's method [25]. The bronze is dissolved in a known amount of 0.1 M $K_3Fe(CN)_6$ solution in alkaline media, then potassium iodine and zinc sulphate are added; the solution is acidified and the excess ferricyanide is estimated with a standardized thio-sulphate solution. It is assumed that just $x$ equivalents of oxidant are necessary to dissolve 1 mol of $Na_xWO_3$. Energy dispersive spectroscopy (EDS) can also be employed for the determination of the sodium content but this needs special standards, software and a highly qualified operator to reach the required accuracy [16]. The most popular method to determine the bronze composition is X-ray powder diffraction (XRD), since the cell parameter of the cubic $Na_xWO_3$ has been shown to vary with the sodium content $x$ as [7, 3]:

$$a = (3.7845 + 0.082 \cdot x)\ [\text{Å}]. \quad (1)$$

The main disadvantage of this method is that it requires a very accurate determination of the cubic

axis which involves prolonged measurements up to high $2\theta$ values ($10^o \le 2\theta \le 140^o$) and an internal standard.

The second goal of this work was therefore to develop an alternative, relatively simple and rapid method of determining $x$ based on the thermogravimetric analysis in an oxidative atmosphere. The method was applied to fine bronze powders synthesized in the framework of the present investigation. An excellent agreement with the $x$ values measured via XRD was found. The proposed method offers for the first time a simple, reliable alternative method of the composition of sodium tungsten bronze.

## Experimental

### Synthesis

The procedure developed and used in this work was based on a thermal reduction process along with gaseous/molten state reaction at high temperature. Different sodium tungsten bronze samples with $x$ associated with the cubic structure were prepared. In the first stage, chemically pure sodium tungstate dihydrate (Fluka), tungsten trioxide in the form of tungstic acid (Riedel-de Haën) and sodium chloride (Frutarom), were heated in an alundum crucible to 800 °C under ambient atmosphere to form a homogenous melt. The chosen temperature was above the melting points of the binary and ternary eutectic points of this system. The first two ingredients had a molar ratio of 1:1, corresponding to $Na_2O{\cdot}2WO_3$, which melts congruently at 738 °C, whereas the NaCl amount was in the 10–40 mol% range. The samples were designated as: B1 (10% NaCl), B2 (20%) and B4 (40%). After cooling, each solidified mixture was ground in a mortar, heated and melted in a tube furnace at 750 °C for 6–60 min in a hydrogen/nitrogen mixture (30 vol% of $H_2$). The gas flow rate was 100 cc/min in order to achieve the thermal reduction process that eventually yielded the bronze:

$$x\mathrm{Na_2WO_{4(m)}} + (2-x)\mathrm{WO_{3(m)}} + x\mathrm{H_{2(g)}} \longrightarrow 2\mathrm{Na}_x\mathrm{WO_{3(s)}} + x\mathrm{H_2O_{(g)}} \quad (2)$$

After cooling, the final product was collected from both the melt surface and the bottom of the crucible. After crystallization, the contents of the crucible were carefully washed on a fine membrane vacuum filter in diluted HCl, ammonia and finally, in distilled water to remove the residues of the starting materials. The separated pure fine bronze powder was dried under ambient conditions.

### Sample characterization

The prepared samples were first characterized visually by their color to roughly determine the range of $x$ in the bronzes. According to [2] the color of the bronze changes from yellow ($x$ = 0.85–0.95) through orange (0.85–0.75) to red (0.75–0.65). The bronze composition was then identified by XRD using a Siemens D5000 powder diffractometer employing $CuK_\alpha$ radiation. The cubic lattice parameters $a$ were determined by least-square fitting of the indexed reflection peaks in the range $10^o \le 2\theta \le 140^o$. The cubic structure was observed for all the samples and the $x$ values (±0.001) were obtained using Brown and Banks' equation allowing the calculation of the composition as a function of lattice parameters [7]. Image analysis of bronze was performed using a SEM (JEOL JSC 5400, Japan) at magnifications of 1000–1500.

Simultaneous thermal and gravimetric analyses (TGA/DTA) were conducted with a Setaram TG-92 unit under flowing air or argon (30 ml/min) at a heating rate of 5 °C/min and a sample mass of 40–50 mg. A novel method of $x$ determination based on the TGA/DTA data was proposed and is presented in this work.

## Results and discussion

The synthesis procedure developed is based on a high temperature gas/melt reaction using hydrogen as a reduction agent. It is suggested that at high temperatures a fast reduction process takes place at the melt/gas interface, causing numerous fine crystals of bronze to form on the melt surface. The crystals grow by transport of tungsten and sodium precursors from the melt to the surface. The growth of crystals is terminated when they precipitate into the melt and leave the hydrogen/melt interface. Precipitation occurs when the gravimetric forces prevail over the surface tension and buoyancy forces of the melt, which oppose the gravitational force. Since the hydrogen diffusion in the melt is negligible, the formation and growth of precipitated crystals is stopped once the crystals settle into the melt. This proposed mechanism is supported by the fact that the bronze particles on the crystallized melt surface, are always found to be smaller than those underneath the melt. In addition, the crystals are found either on the top surface of the melt or on the bottom of the crucible. This suggested mechanism enables control of the crystal size

by changing the melt surface tension, viscosity and density. For example, small crystals can be produced if they are forced to precipitate into the melt at an earlier stage. It is known that addition of NaCl to the melt lowers the surface tension, density and viscosity of ternary melts used in the present work [26–29]. Therefore, to prove the suggested mechanism above, we added different amounts of sodium chloride to the melt and inspected the effect on the crystals. The obtained bronze crystals are cubic, in good agreement with the determined value of $x$. The cubic structure is characteristic for sodium tungsten bronzes with $x > 0.4$ [2].

The particles' size obtained at 10, 20 and 40% NaCl concentration is shown in the SEM micrographs in Fig. 1a, b, c, respectively. These images clearly show the decrease of bronze crystal size with the increase of NaCl concentration in the melt. In addition, a change from a bimodal size distribution to a monomodal one is also observed. As seen in Fig. 1a, at 10% NaCl the measured bimodal size range was 2.5–3.5 μm with an average of 3 μm for the smaller fraction and 9–18 μm with an average of 13 μm for the larger fraction of crystals. At 20% NaCl the measured bimodal size range was 2–3 μm with an average of 2.4 μm for the smaller fraction and 6–8.5 μm with an average of 6.5 μm for the larger fraction of crystals. And finally, Fig. 1c shows that for 40% NaCl the measured size range was 2–5 μm with an average of 3.2 μm. The difference between the large and small fractions of particles also decreases with the increasing content of NaCl. At 10% NaCl the difference in size between the fractions was about 10 μm, while for 20% it was about 4 μm and it could no longer be observed for 40% NaCl. These results from image analyses are correlated well with the suggested influence of the melt surface tension, density and viscosity on the yielded bronze crystals: the presence of sodium chloride lowers the melt surface tension, density and viscosity, which in turn allows the crystals to settle into the melt at an earlier stage, thus decreasing the crystal size and changing the size distribution.

The suggested mechanism predicts that the synthesis time should not affect the final particle size of the bronze crystals. This fact is evident by images of the bronze powders obtained during 6–60 min at 750 °C, as shown in Fig. 2a, b, c. As seen in Fig. 2a, b, c, the crystals sizes obtained in the 6–60 min of reaction are very similar. Therefore, the morphology of bronze powders seen in Fig. 2a, b, c was controlled by the melts' surface tension, density and viscosity rather than by the synthesis time, consistent with the suggested mechanism.

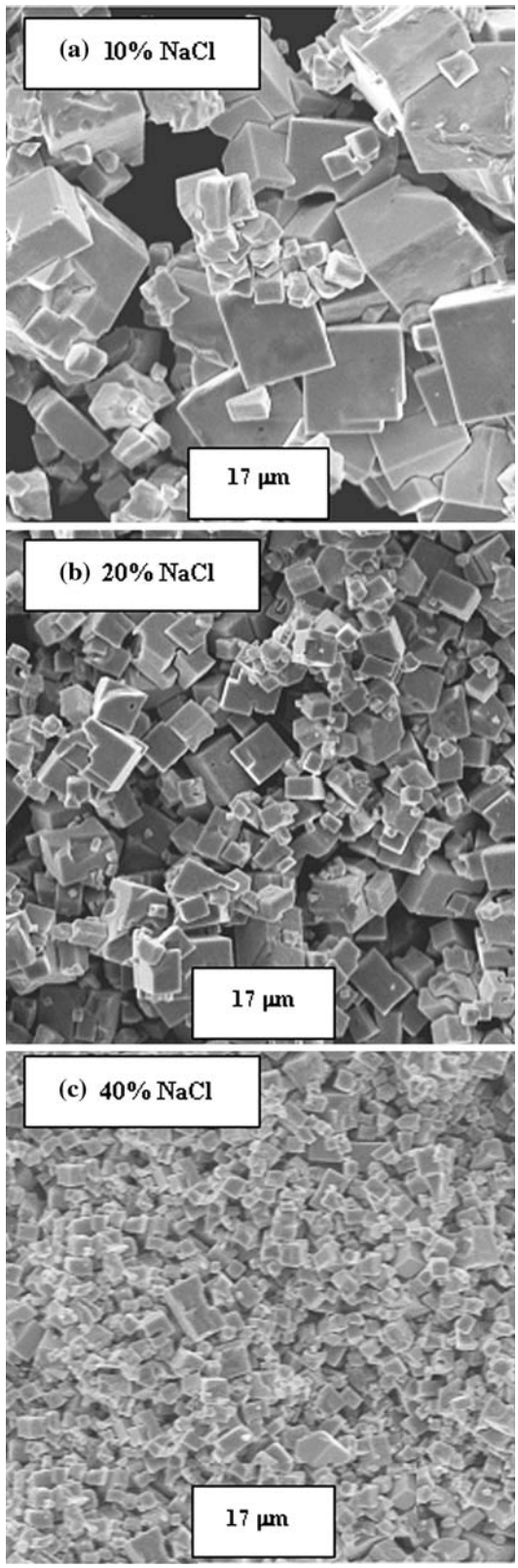


**Fig. 1** SEM micrographs of bronze cubic powder (at ×1,500) synthesized in melts with (**a**) 10% (**b**) 20% and (**c**) 40% NaCl at 750 °C for 18 min

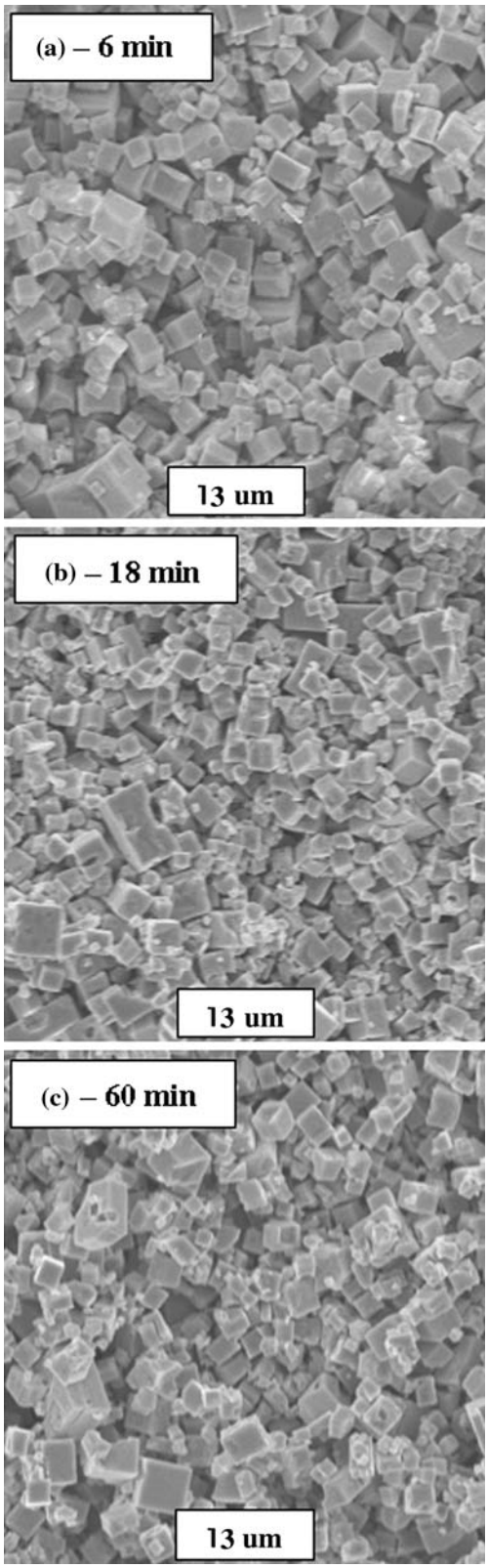


**Fig. 2** SEM micrographs of bronze cubic powder (at ×2,000) synthesized in melts with 40% NaCl at 750 °C for different times: (**a**) 6 min; (**b**) 18 min; (**c**) 60 min

The thermal behavior of the bronze crystals was investigated by thermogravimetric analysis. Typical TGA curves in air or argon atmospheres for pure powders of sodium tungstate bronzes, synthesized in melts with different contents of sodium chloride, are presented in Fig. 3. The TGA data obtained under argon indicated a weight stability of the bronzes at least until 800 °C. No drastic changes in weight were observed and no thermal effects were detected on DTA curves. Therefore, it can be concluded that the synthesized bronzes have a good thermal stability in the investigated temperature range in a non-oxidative atmosphere. In contrast to the stable pattern in argon, the pattern in air, shown in Fig. 3, includes three separate zones:

(a) A low temperature zone, up to 390 °C where no weight gain or DTA effects are observed.

(b) An intermediate zone at 390–700 °C, where a weight gain of 2.5–3 wt% occurs. The DTA curves indicate a wide indistinct exothermic effect between 450 °C and approximately 680 °C. This effect is related to the process of the Sodium Tungsten Bronze (STB) oxidation by air oxygen, above a certain temperature, as described by Eq. 3.

$$2 \cdot Na_xWO_{3(s)} + \frac{x}{2} \cdot O_{2(g)} \rightarrow x \cdot Na_2WO_{4(s)} + (2-x) \cdot WO_{3(s)} \quad (3)$$

(c) A high temperature zone above 700 °C, where the weight becomes stable again.

The insert of Fig. 3 shows a DTA curve of bronze synthesized with 20% NaCl. The DTA measurement was made simultaneously with the TGA, under air atmosphere.

A well distinct, strong endothermic effect at 735 ± 5 °C was determined from the DTA curves shown in Fig. 4. This sharp peak is associated with the melting process of the products yielded from the oxidation of bronze in the intermediate zone (b). At the end of this zone the bronzes undergo complete oxidation and from this moment on they do not exist any more. According to Eq. 3 sodium tungstate and $WO_3$ should be obtained as products and precisely a mixture of these compounds are melted at temperatures above ~700 °C. This is correlated with the white color of the crystallized products observed in the TGA/TDA crucible after air treatment at 750 °C. The melting process might be described in terms of the binary phase diagram of the $Na_2WO_4$–$WO_3$ system [30]. The ratio between the components is a function

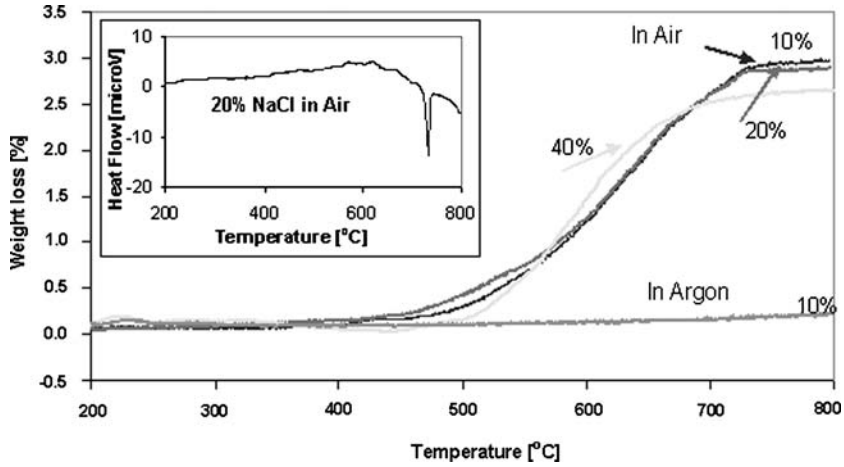


**Fig. 3** TGA of bronze synthesized at different NaCl concentrations. Insert: DTA of bronze synthesized with 20% NaCl

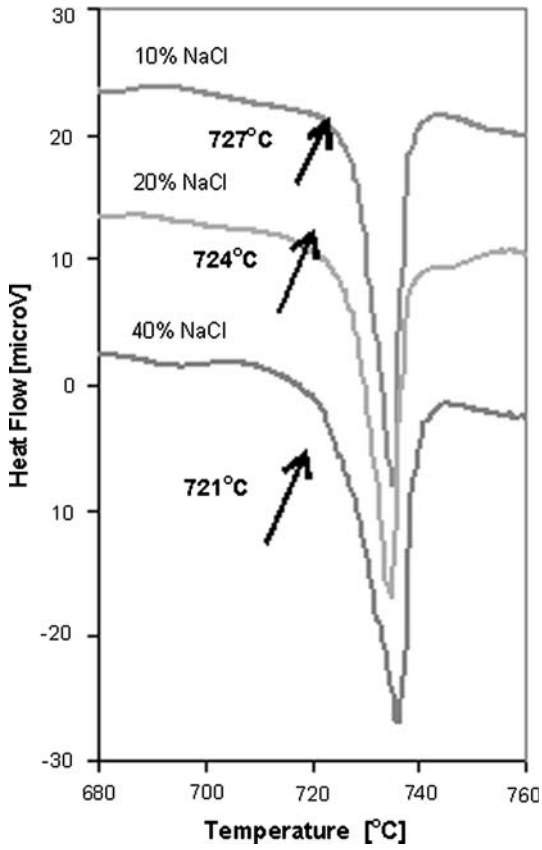


**Fig. 4** DTA of bronze synthesized at different NaCl concentrations: range of melting

of the value of $x$ in heated bronze, as seen in Eq. 3. For example, a value of 0.9 for $x$ ($Na_{0.9}WO_3$), would yield a $Na_2WO_4$:$WO_3$ ratio of 45:55 mol%, respectively. The melting point for this mixture is matched to the liquidus temperature in the area denoted "$L$" in the phase diagram at ~55 mol% of $WO_3$. It indicates an agreement between the melting point temperatures and the products ratio as calculated from Eq. 3 and detected by DTA measurements. To explain the bronze melting process effectively we reproduced the $Na_2WO_3/WO_3$ phase diagram from the literature [30] and inserted it in Fig. 5. According to the phase diagram and the components ratio, the crystallized matter should contain $Na_2W_2O_7$ and $Na_2W_4O_{13}$ instead of $Na_2WO_4$ and $WO_3$. Sodium ditungstate and sodium tetratungstate are the congruently and incongruently melted phases, respectively (Fig. 5) and their ordinates divide the solidus part of phase diagram into three sections: (1) $Na_2WO_4$–$Na_2W_2O_7$, (2) $Na_2W_2O_7$–$Na_2W_4O_{13}$ and (3) $Na_2W_4O_{13}$–$WO_3$. Because the $x$ value in bronze is always <1, the ratio between the products in Eq. 3 has to be $x$:$(2-x)$, hence the $WO_3$ fraction is always larger than that of $Na_2WO_4$. Therefore, the products of bronze oxidation are crystallized in Sects. "Experimental" or "Results and discussion" of the phase diagram (Fig. 5). When $x > 0.5$, which is characteristic of the investigated bronzes, the ratio between the final phases is located in Sect. "Experimental" of the diagram (Fig. 5). In other words, along with the chemical process of the bronze oxidation, a high temperature phase formation of $Na_2W_2O_7$ and $Na_2W_4O_{13}$ has occurred. The presence of sodium ditungstate and tetratungstate was proved by XRD analysis shown in Fig. 6. The XRD pattern includes some gold (Au) lines, which was used as an internal standard for measurement of the peaks' position of $Na_2W_2O_7$ and $Na_2W_4O_{13}$. Therefore, the final equation, of the bronze oxidation process can be written as follows:

$$\begin{aligned} 2\cdot Na_xWO_{3(s)} + \frac{x}{2}\cdot O_{2(g)} &\longrightarrow x\cdot Na_2WO_{4(s)} \\ &+ (2-x)\cdot WO_{3(s)} x\cdot Na_2WO_{4(s)} \\ 2\cdot Na_xWO_{3(s)} + \frac{x}{2}\cdot O_{2(g)} &\longrightarrow (2x-1)\cdot Na_2W_2O_{7(s)} \\ &+ (1-x)\cdot Na_2W_4O_{13(s)} \end{aligned} \quad (4)$$

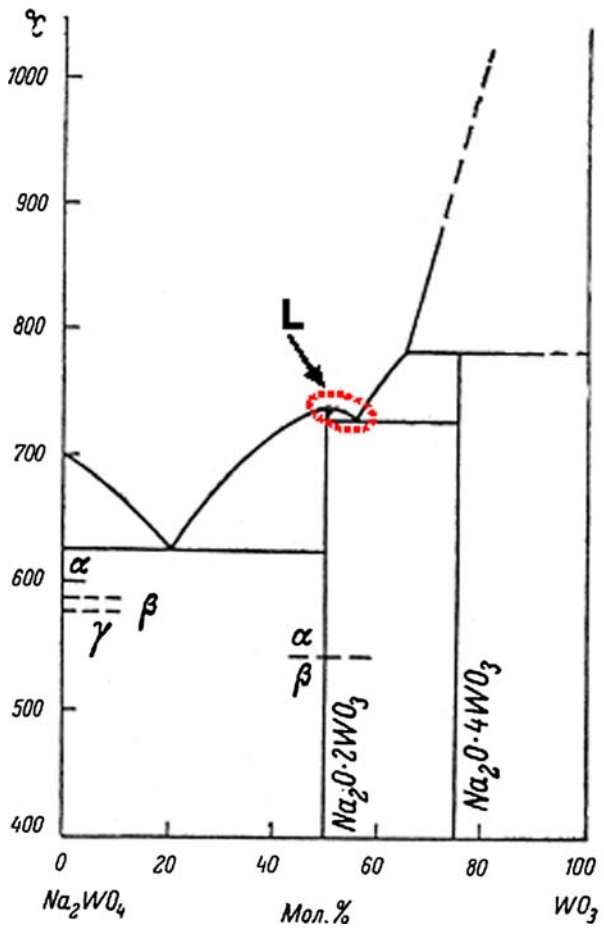


**Fig. 5** Phase diagram of the bronze melting products, reproduced from [30]

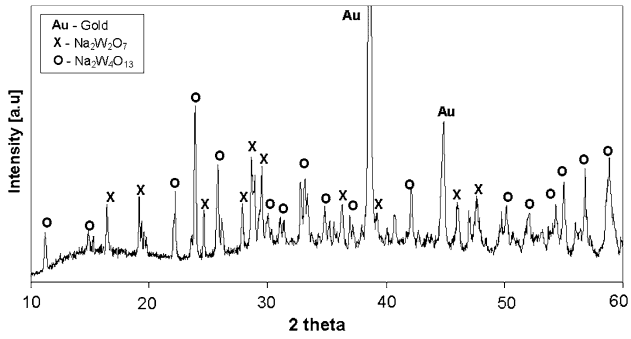


**Fig. 6** XRD spectrum for crystallized melt of oxidized bronze

In Fig. 4 three endothermic peaks of melting are presented and each of them is associated with a bronze synthesized in the melt with a different NaCl content: 10, 20 and 40 mol%. As illustrated in Fig. 4, the melting is shifted towards lower temperatures as the NaCl content increases. This phenomenon can be explained by the effect of the NaCl content on the value of $x$ (Table 1), and in turn on the ratio between sodium ditungstate and $WO_3$. The rise of the NaCl content causes a decrease in the value of $x$ for bronzes and a change of the components' ratio in the final product after bronze oxidation in melt. When this ratio is changed the liquidus temperature is also changed (see Fig. 5), consistent with the DTA curves of Fig. 4. The measured melting points decreased from 727 °C to 721 °C and this correlates with the lowering of liquidus in area $L$ with the increase of $WO_3$. This can occur only in the case when the value of $x$ in Eq. 4 decreases.

The second aim of this work was the development of a simple, yet accurate method to determine the bronze composition. A novel and simple method for the determination of the sodium content (the value of $x$) is based on the TGA data in the intermediate zone (b) that is related to the bronze oxidation process. To demonstrate this method a known, accurate amount of synthesized and purified STB was placed in the TGA/DTA crucible and heated linearly to about 800 °C. A typical TGA pattern is obtained and shown in Fig. 3. The samples' weight gain (WG) is measured between the end of zone (a) at ~390–395 °C and the end of zone (b). This weight gain represents the exact weight of oxygen taken up by the bronze oxidation according to Eq. 3. Using the determined WG, a calculation of the exact amount of oxygen moles that is equal to $x/2$ (Eq. 3) can easily be performed with high accuracy that is dependent on the precision of the TGA experiment. In this way, the $x$ values for numerous samples of bronzes were calculated from the WG measured by TGA. Examples of the results obtained for bronzes synthesized for different NaCl contents are presented in Table 1.

In order to verify the accuracy of the method, the value of $x$ was also calculated from the XRD determination of the $a$ lattice parameter of the crystals [7]. The XRD experimental data is shown in Fig. 7. In order to perform the XRD measurements with the required accuracy a slice of gold foil was placed in the powder to serve as an internal standard for fine calibration of the spectra. The values of $a$ were determined by least-squares fitting of the reflection peaks in the range. The estimated standard deviations of the calculated $a$ axes were all 0.001 Å. The gold peaks are marked in Fig. 7a and one can notice that there was no shift in the position of the gold peaks between the three samples. The rest of the peaks reflect the bronzes' patterns. Since the samples were synthesized in the melt with different NaCl contents, the effect on the XRD patterns was examined. A slight shift towards the larger angles (Fig. 7b, c) is observed with the increasing sodium chloride content. Magnifications of two

**Table 1** Comparison between the values of $x$ obtained from the TGA and XRD data

| NaCl (%) | TGA | XRD | | Divergence between $X_{TGA}$ and $X_{XRD}$ (%) | Bronze color |
|---|---|---|---|---|---|
| | $X_{TGA}$ | $a$ (Å) | $X_{XRD}$ | | |
| 10 | 0.912 | 3.859 | 0.907 | 0.50 | Yellow |
| 20 | 0.851 | 3.854 | 0.847 | 0.53 | Orange |
| 40 | 0.809 | 3.850 | 0.798 | 1.38 | Orange-red |

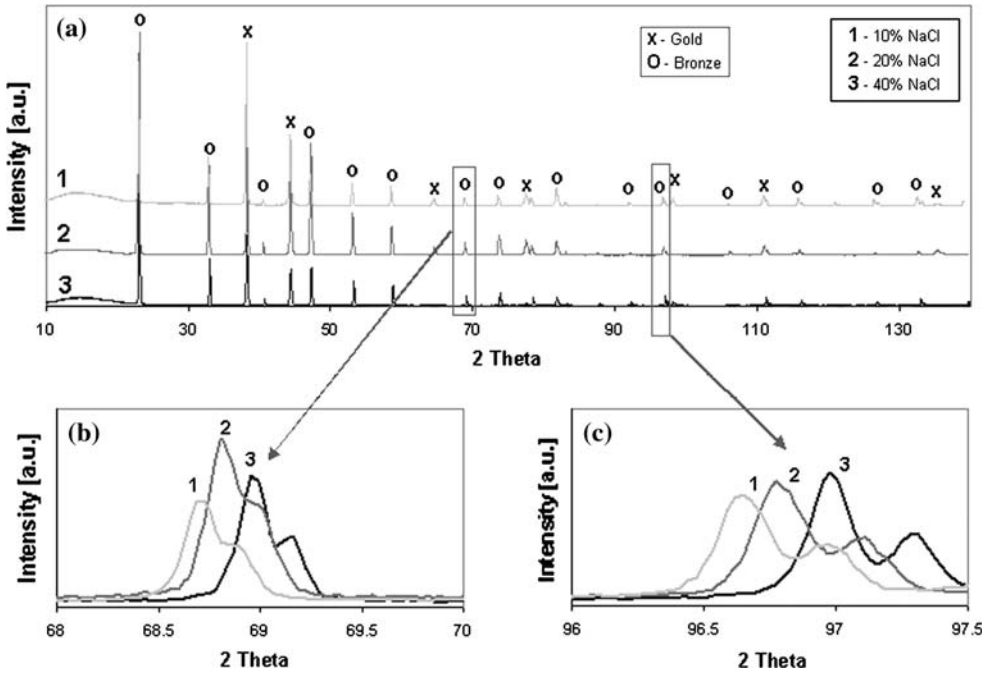


**Fig. 7** XRD spectra for the bronze samples: (**a**) the entire spectrum; (**b**) and (**c**) a magnification of two parts, showing the shift of characteristic bronze peaks

parts of the XRD spectra are shown in Fig. 7b, c and present the shift of the same typical bronze peaks (indexed as (220) and (321), respectively) of three samples. This shift is associated with a change in the value of the cell constant $a$ which is a function of $x$ of the investigated bronzes. The lattice constant $a$ (cubic pervoskite structure) was calculated for each sample, and from it $x$ was obtained using Eq. 1. Results are presented in Table 1, where the first column is the NaCl content in the melts from which the bronzes were synthesized. $X_{TGA}$ is the value of $x$ obtained by TGA route. The bright colors of the bronzes are a characteristic of these $x$ values. The colors of samples fit the earlier observed colors for different bronzes [2]. Finally, the content of sodium in the synthesized bronzes was found to be in the range of about 0.81–0.91 by TGA and 0.80–0.91 by XRD. As can be clearly seen from Table 1, an excellent agreement between the values of $x$, calculated via the TGA and XRD data, has been achieved. The difference between the $x$ values calculated by the proposed TGA method and the classical XRD method was found to be in the range of 0.5–1.5%.

## Conclusions

The synthesis of fine powders of tungsten inorganic bronze by a high temperature gas/melt reduction process was developed and investigated in the present work. A melt of sodium tungstate and $WO_3$ in the molar ration of 1:1 with additives of sodium chloride varied from 10 mol% to 40 mol%. were used as high temperature medium for bronze formation and flowing hydrogen was utilized as reduction agent at 750 °C. The developed procedure allows control of the particle size and its distribution. An increase in NaCl content leads to decrease of crystals size and improves the powder uniformity. The $x$ value slightly decrease with NaCl addition, but it still remains in the upper scale range ($x > 0.8$) of high symmetric cubic yellow-orange bronzes even at high sodium chloride content of 40 wt%. Fine powders in the 2–5 μm size range were synthesized from melt with 40 mol% of NaCl. An original mechanism of controlling the powders size was suggested and discussed.

A novel, accurate and simple method to determine the bronze composition ($x$ value), based on thermo-

gravimetric analysis in oxidative atmosphere, was developed. The stoichiometry parameter $x$ of obtained bronzes ranged from 0.8 to 0.92. The principle of $x$ calculation through quantitative TGA measurements was explained. An excellent agreement between $x$ values measured by the classical XRD route and the proposed TGA route was demonstrated.

Both synthesis procedure and $x$ determination method developed in present work could be utilized for variety types of inorganic bronzes such as tungsten, molybdenum, vanadium bronze of alkali and alkaline earth metals.

**Acknowledgements** The investigations were supported by the Technion's fund for the promotion of research and in part by a joint grant from the Center for Adsorption in Science of the Ministry of Immigrant Absorption State of Israel and the Committee for Planning and Budgeting of the Council for Higher Education under the framework of the KAMEA Program.

## References

1. Philipp J, Schwebel P (1879) Ber Deutsch Chem Ges 12:2234
2. Edwards PP, Rao CNR (1985) The metallic and nonmetallic states of matter. Taylor & Francis
3. Hagenmuller P (1971) In: Progress in solid state chemistry, vol 5. Oxford Pergamon, p 71
4. Sienko MJ (1963) In: Non-stoichiometric compounds. Advances in Chemistry Series, American Chemical Society, p 224
5. Ribnick AS, Post B, Banks E (1963) In: Non-stoichiometric compounds. Advances in Chemistry Series, American Chemical Society, p 246
6. Randin JP (1974) J Chem Educ 51(1):32
7. Brown BW, Banks E (1954) J Am Chem Soc 76:963
8. Barabushkin AN, Kaliev KA, Vakarin SV, Dokuchaev LYa, Butrimov VV, Aksent'ev AG (1988) U.S.S.R., SU 1425531 A1 19880923
9. Ozerov RP (1954) Uspekhi Khimii 24:951
10. Shanks HR (1972) J Crystal Growth 13/14:433
11. Bartha L, Kiss AB, Szalay T (1995) Int J Refractory Metals & Hard Mater 13(1–3):77
12. Shurdumov BK (2001) Izvestiya Vysshikh Uchebnykh Zavedenii, Khimiya i Khimicheskaya Tekhnologiya 44(6):152
13. Shurdumov BK, Shurdumov GK, Kuchukova MA (1999) RU 2138445C1
14. Salje E, Hatami H (1973) Z Allg Chem 396:267
15. Zhu YT, Manthiram A (1994) J Solid Sate Chem 110:187
16. Fan R, Chen XH, Gui Z, Li SY, Chen ZY (2001) Mat Let 49:14
17. Dickens PG, Whittingham MS (1965) M S Trans Faraday Soc 61:1226
18. Weber MF, Bevolo AJ, Shanks HR, Danielson GC (1981) J Electrochem Soc 128(5):996
19. Bevolo AJ, Weber MF, Shanks HR, Danielson GC (1981) J Electrochem Soc 128(5):1004
20. Shanks HR, Bevolo AJ, Danielson GC, Neker MF (1980) Fuel cell oxygen electrode, U.S. Pat. Appl. US 18211
21. Binder H, Knoedler R, Koehling A, Sandstede G (1977) Device for the continuous determination of carbon monoxide content in air, U.S. Pat. Appl. US 580532
22. Wechter MA, Hahn PB, Ebert GM, Montoya PR, Voigt AF (1972) Anal Chem 45:7
23. Hahn PB, Wechter MA, Jhonson DC, Voigt AF (1973) Anal Chem 45:7
24. Whittimgham MS, Huggins RA (1971) J chem Phys 54:1
25. van Duyn D (1942) Recl Rtav Chim Pays-Bas, Belg 61:661
26. Cleaver B, Koronaios P (1994) J Chem Eng Data 39(4):848
27. Khakulov ZL, Mohosoev MV, Vorozgbit VU, Shurdumov GK (1983) Khimia I Tekhnol Molibdena I Vol'frama, Nal'chik, USSR 7:23
28. Vorozgbit VU, Shurdumov GK, Kodzokov KhA (1979) Khimia I Tekhnol Molibdena I Vol'frama, Nal'chik, USSR 5:79
29. Shurdumov BK (1976) Khimia I Tekhnol Molibdena I Vol'frama, Nal'chik, USSR 3:175
30. Hoermann F (1928) Zs Anorgan Allgem Chem 177(2–3):145; Tropov NA, Barzakovsky VP, Lapin VV, Kurtseva NN (1969) Phase diagrams of silicates systems. Academy of Science USSR, ''Nauka'', Leningrad, p 628